

EMI from Airflow Aperture Arrays in Shielding Enclosures

Min Li

Electromagnetic Compatibility Laboratory
University of Missouri-Rolla
mili@ece.umar.edu

I. Introduction

The integrity of shielding enclosures is compromised by aperture arrays for heat dissipation. Radiation from slots can usually be minimized with gasketing. However, it is more difficult to mitigate the radiation from intended apertures. Enclosures for high-speed digital designs use perforated metal sheets instead of large open apertures for airflow and heat dissipation. Structural and heat dissipation requirements place a lower bound on the size of the apertures in the perforation pattern. This bound may lead to EMI problems at high frequencies. A closed-form expression, or empirical approach for airflow aperture array design is desirable for quick engineering calculations.

A rectangular test enclosure with faces accommodating different aperture arrays was investigated experimentally and with FDTD modeling. MoM modeling was also utilized to study the nature of aperture radiation as a function of mutual coupling. The modeling results from three aperture arrays were corroborated with measurements. A simple design equation can be proposed for relating the EMI from aperture arrays to the size and numbers of the apertures. The simple design equation agrees well with the measurements, and the numerical modeling results.

II. Problem Description

A shielding enclosure mimicking an actual product enclosure for a file server is shown in Figure 1. The interior dimensions of the enclosure were $20\text{ cm} \times 40\text{ cm} \times 50\text{ cm}$. A 0.1 cm thick plate was used for the face containing the aperture array (except that in the case of the smallest aperture array where a 0.165 cm thick aluminum plate was used for machining purposes). Three aperture arrays, with aperture sizes of $1\text{ cm} \times 1\text{ cm}$, $1.5\text{ cm} \times 1.5\text{ cm}$, $2.05\text{ cm} \times 2.05\text{ cm}$, and spacings of 0.5 cm , 1.0 cm , 1.0 cm , respectively, were investigated experimentally. The 2.05-cm aperture size as opposed to 2 cm was chosen due to restrictions on the geometry in the FDTD modeling. The number of apertures for these three aperture arrays was 252, 112, and 60, respectively. A terminated feed probe at $x=43\text{ cm}$, $z=33\text{ cm}$ was employed as an excitation source. The center conductor of the probe was extended to span the width of the cavity with a 0.16-cm diameter wire, and terminated on the opposite cavity wall with a 1206 package size surface-mount (SMT) nominal 47Ω resistor soldered to a $1.5'' \times 1.5''$ square of conductive adhesive copper tape. A layer of $110\Omega/\text{square}$ lossy material (Milliken Contec) with a thickness of approximately 1.0 cm was placed against the $x=50\text{ cm}$ wall to reduce the artificially high Q of the enclosure.

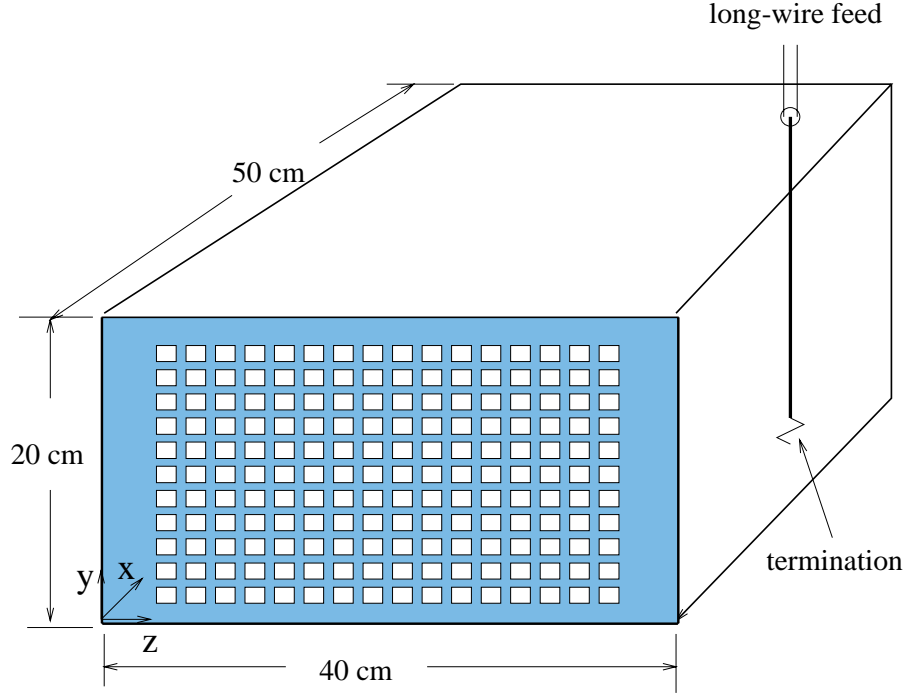


Figure 1. The geometry of the test enclosure.

The finite-difference time-domain (FDTD) method was employed to model the test enclosure excited by a terminated feed probe. Two additional aperture arrays, with aperture sizes of $2.5\text{ cm} \times 2.5\text{ cm}$, and $3\text{ cm} \times 3\text{ cm}$, aperture spacings of 1.5 cm , and 2.0 cm , and aperture numbers of 44, and 28, respectively, were also studied in the FDTD modeling in addition to the geometries investigated experimentally. A cell size of $0.5\text{ cm} \times 0.5\text{ cm} \times 1.0\text{ cm}$ was employed in the FDTD modeling for all configurations except that a cell size of $0.51\text{ cm} \times 0.51\text{ cm} \times 1.0\text{ cm}$ was used for the $2.05\text{-cm} \times 2.05\text{-cm}$ aperture configuration. Aluminum plates were modeled with perfect electric conducting (PEC) surfaces by setting the tangential electric field to zero on the cavity walls. The wire feed-probe was modeled using a thin-wire algorithm [1]. The source was modeled by a simple voltage source V_s , with a 50Ω resistance incorporated into a single cell at the feed point. The magnetic fields circling the source were modeled in the same fashion as a thin wire to give the cross-section of the source a specified physical dimension [2]. The resistor was modeled as a lumped element using a subcellular algorithm [3]. The width of the SMT resistor is approximately that of the feed wire diameter and the physical cross-section dimensions were modeled with the same diameter as that of the feed wire by modifying the magnetic field components circling the SMT in the same fashion as for the source. Thin slots were modeled with the capacitive thin slot formalism (C-TSF) introduced by Gilbert and Holland [4], as applied to shielding enclosures [5]. The lossy material was simply modeled by a one-cell layer of conducting material with conductivity $\sigma = 0.0227\text{ S/cm}$. For the electric field components inside the conducting layer, the conductivity $\sigma = 0.0227\text{ S/cm}$ was employed, while the conductivity $\sigma = \frac{0.0227}{2}\text{ S/cm}$ was employed for the components on the interface of the conducting layer and free space [1]. Perfectly-Matched-Layer (PML) absorbing boundary conditions were

employed for the 3D FDTD modeling [6]. The PML absorbing layers were 4 cells away from the conducting planes without the apertures, and 8 cells away from the conducting plane containing the apertures. A time history of $10,000$ time steps was recorded in all the FDTD modeling, and an additional $80,000$ steps were extrapolated using Prony's method [7]. The far-zone field was obtained by applying equivalence theory to the FDTD modeling results [8].

The MoM was used to better understand the coupling between apertures, and as a basis for correction factors in the FDTD results due to inadequate discretization in the apertures. The problem was formulated for apertures in an infinite conducting screen [9]. MoM using triangle basis functions and a Galerkin's procedure was employed herein to obtain the equivalent magnetic surface current density $\vec{M}(\vec{r})$ in the apertures [11]. Assuming the footprint of the aperture array is much smaller than the distance $R=3\text{ m}$, and the apertures are closely spaced relative to a wavelength (which is generally satisfied), the expression for $|E_{3m}|$ can be reduced to

$$|\vec{E}_{3m}| \approx \frac{\epsilon\omega}{2\pi R} |\vec{M}_i(\omega)| \quad (1)$$

where $|\vec{M}_i(\omega)| = |\iint \vec{M}(\vec{r}', \omega) ds'|$ for each aperture or aperture array. Since the equivalent magnetic surface current density vector in the aperture is directly proportional to radiated EMI, $|\vec{M}_i|$ can be used to study the effects of aperture coupling on EMI.

S-parameters and radiated EMI measurements were performed in a 3-m anechoic chamber. Two-port S-parameters were measured with a Wiltron 37247A network analyzer. Port 1 was connected to the interior source in the enclosure under test, and Port 2 was connected to a log-periodic dipole array ($200\text{ MHz} - 5\text{ GHz}$) receiving antenna. The network analyzer was placed outside the anechoic chamber to measure the transmission coefficient $|S_{21}|$. Far-zone electric field measurements were made with a separation of 3 m between the enclosure and the receiving antenna. The far-zone electric field provides a quantitative measurement of the levels of EMI and is related to the S-parameters by [11]

$$E_{3m} = AF \times |S_{21}| \times 0.5V_s \quad (2)$$

where AF is the antenna factor of the receiving antenna, and V_s is the source voltage with $50\text{-}\Omega$ source impedance.

III. Results and Discussion

Measurements and FDTD modeling were used to investigate the 1.0-cm , 1.5-cm , and 2.05-cm aperture arrays. Radiated measurements were made to corroborate the modeling on 1.0-cm , 1.5-cm , and 2.05-cm aperture arrays. A comparison between the modeled and radiated electric field measurements is shown in Figure 2. The effect of a non-zero aluminum plate thickness, t_c , for the panel containing the aperture array was considered by using an empirical estimate for the attenuation of $32 \frac{t_c}{d}$ (dB) (d is the diameter of a circle having the same area as a single square), to scale the measured results to a zero-

thickness plate, for direct comparison with the modeling [12]. The attenuation factors were 4.7 dB for the 1-cm aperture array, 1.8 dB for the 1.5-cm aperture array, and 1.3 dB for the 2.05-cm aperture array.

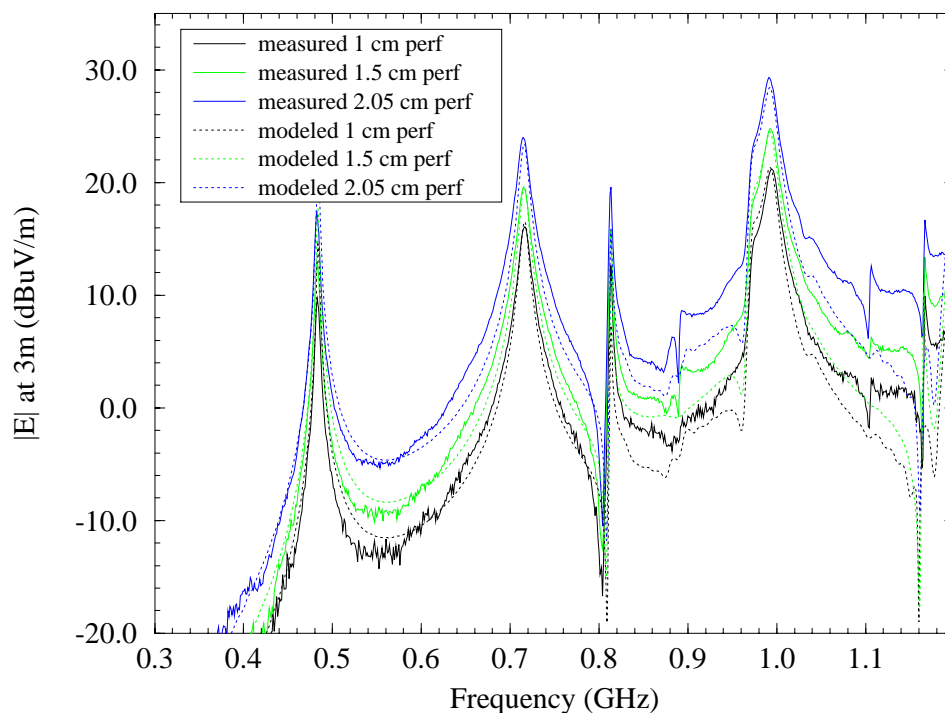


Figure 2. The comparison between measurements and FDTD modeling of aperture arrays in the test enclosure.

A compensation procedure, based on a comparison between FDTD and MoM modeling results, was developed to compensate for the effect of an inadequate number of cells, and different cell numbers in the apertures. The correction procedure was carefully done based on a comparison between the FDTD modeling, measurements and MoM modeling, and was not a scaling number for the purpose of good agreement [8]. The MoM modeling approach, as used herein, had over 200 mesh elements per aperture with a finer sampling near the periphery of the aperture. The MoM results for a single aperture while varying the aperture size from 1 cm to 3 cm indicate a relation of $EMI \propto a^3$ (a is the length of one side of the square aperture), i.e., the far field radiation from an aperture is proportional to a^3 at frequencies well below the aperture resonances. This is consistent with the Bethe small-hole theory [13]. Measurements were also performed on the radiation from a single aperture cut from copper tape covering a 3-cm aperture. The results corroborate the relation of EMI to the aperture size $EMI \propto a^3$ for a single aperture. The overall correction factors were 3.0 dB , 4.0 dB , 5.5 dB , 8.0 dB , and 12.0 dB for the 3.0-cm , 2.5-cm , 2.05-cm , 1.5-cm , and 1.0-cm apertures, respectively. All the FDTD radiated field modeling results presented herein were corrected by these factors.

The agreement after scaling the measurements for the plate thickness is generally good, except for frequencies near 1.2 GHz . This discrepancy may be due to neglecting the frequency dependent characteristic of the lossy material in the FDTD modeling. The shape of the frequency response for the electric field strength is the same for all the

aperture arrays, indicating that the power radiated through the aperture arrays is only a small fraction of the power delivered to the enclosure, and that there are no aperture resonances in the frequency range studied.

A simple equation for the relation between EMI, the aperture size, and the number of apertures is useful in shielding enclosure design. The EMI as a function of aperture size for a single aperture was studied using MoM modeling, and an a^3 relation was obtained. The mutual coupling between apertures was investigated by FDTD modeling and MoM to obtain a relationship between radiated emissions and the number of apertures.

The aperture mutual coupling was also studied with MoM to understand the variation of radiated field with the number of apertures N and the aperture spacing. Here, plane wave incidence was assumed, the apertures were in an infinite conducting plane, and a 3×3 aperture array was investigated to ascertain the coupling effect on the center aperture. A coupling coefficient C_m for each aperture is defined as

$$C_m = \frac{M_t^{multiple} - M_t^{single}}{M_t^{single}}, \quad (3)$$

where $M_t^{multiple}$ is for one aperture in an aperture array, and M_t^{single} is for a single aperture. The aperture size was $2 \text{ cm} \times 2 \text{ cm}$, and the frequency was 1 GHz . The coupling coefficient as a function of aperture spacing is shown in Figure 3. The result is comparable to one aperture in a large aperture array, since the mutual coupling effects will be dominated (for EMI purposes) by the eight apertures immediately adjacent to it. The mutual coupling from an aperture with a spacing greater than the size of the aperture (but significantly less than a wavelength) was negligible.

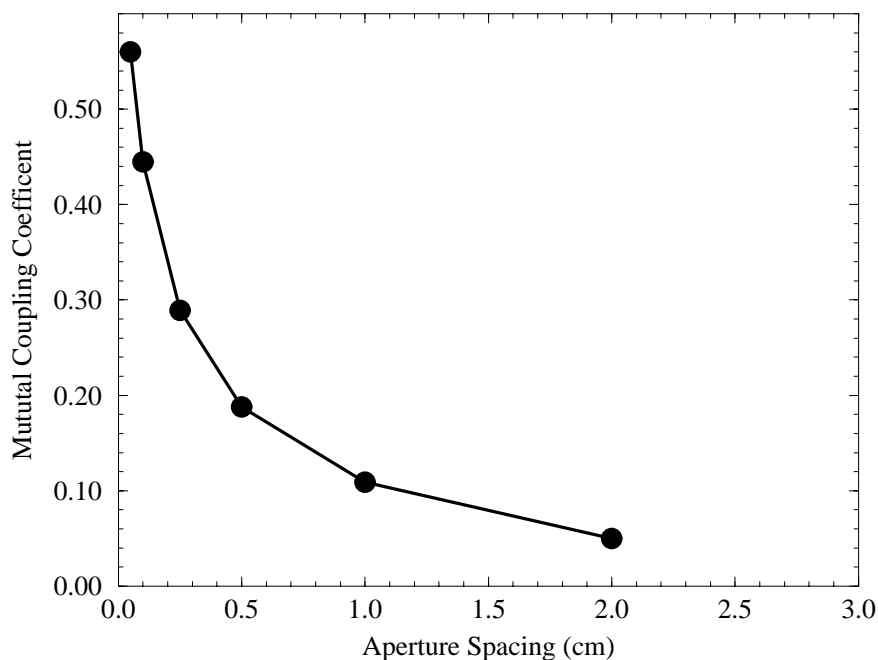


Figure 3. The mutual coupling for the aperture in the middle of a nine aperture array.

The mutual coupling between apertures is generally negligible if the spacing between apertures is not small compared to the aperture size. For the cases studied above, the spacing of half of the aperture size for an aperture array yielded a mutual coupling coefficient of 0.11 . The array of 252 apertures will generate an EMI of $252 \times 1.11 \times e_i$ (e_i is the field from an individual aperture, the aperture fringing effect is neglected) compared to the summation of EMI from 252 individual apertures, or $252 \times e_i$. The difference is only 1 dB , and indicates a scaling with N for the EMI from aperture arrays in a shielding enclosure.

Radiation measurements for an increasing number of 1-cm apertures in an aperture array (9 to 252 apertures) on one face in the test enclosure are shown in Figure 4, for the frequency range from 0.3 GHz to 1.2 GHz . The results indicate that the radiation is directly proportional to the number of apertures N . The aperture size was 1 cm , and the aperture spacing was 0.5 cm , denoted as “dense apertures” in Figure 4. The number of apertures was varied by masking a portion of the total aperture array ($N=252$) footprint with copper tape. The aperture configurations tested always had the array located symmetrically about the center in the front panel. The apertures were oriented along a constant grid pattern from row-to-row, as opposed to being offset by one-half the spatial periodicity. The offset aperture arrays were also investigated with FDTD modeling, and the results for the delivered power and EMI were the same as those for the aperture arrays with no offset, within 0.5 dB . The frequency range of the measurements was 0.3 GHz to 1.2 GHz . The variation in the radiation with aperture number was found to be uniform over the entire frequency range.

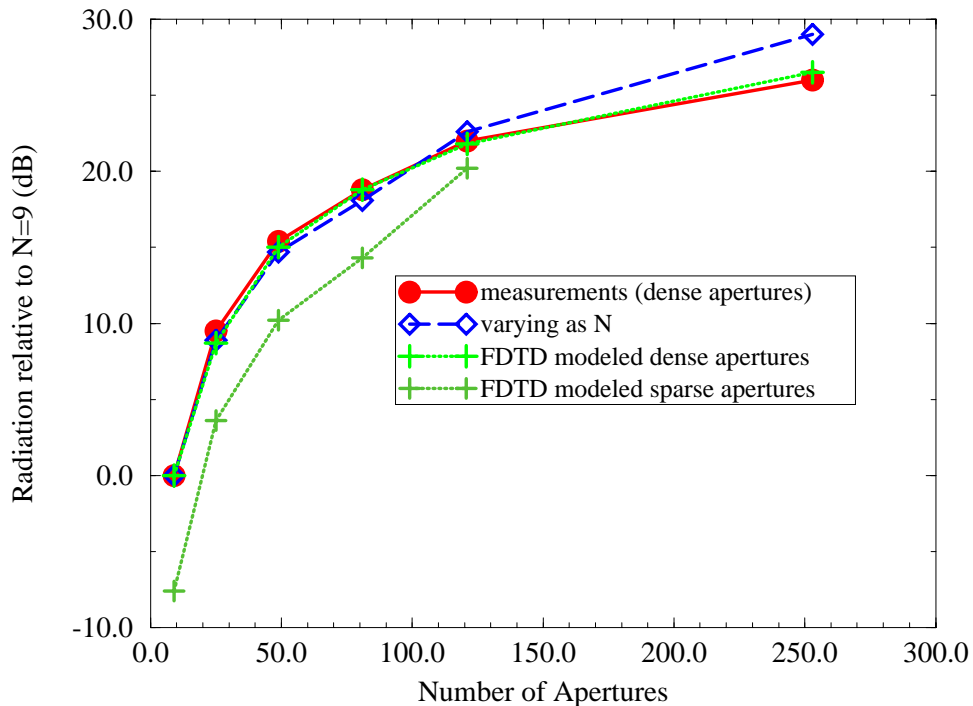


Figure 4. The radiation from multiple apertures for 1-cm apertures in the test enclosure.

As a conclusion, a design approximation for the radiation from aperture arrays in a shielding enclosure is $|E| \propto Na^3$ for arrays with aperture spacing not small compared to the aperture size. A comparison between the $|E| \propto Na^3$ variation and measurements and FDTD modeling is shown in Figure 5. for the five aperture arrays studied. The results are based on the frequency range of 0.3 GHz to 1.2 GHz. Here the FDTD results have been corrected for the aperture cell-number based on comparing the measurements, the FDTD results, and MoM results as described above. Since only three array panels were available experimentally, the “experiment” curve for larger aperture sizes was extended using FDTD modeling based on the methods described above.

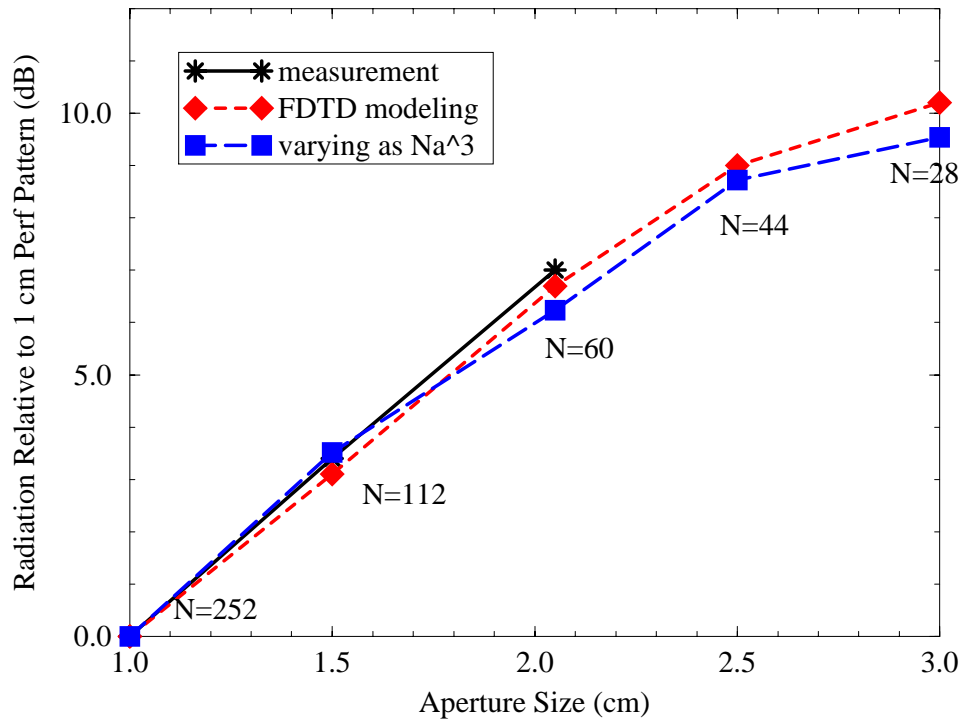


Figure 5. Measured and FDTD modeled radiation from aperture arrays and the empirical approach.

References

- [1] A. Taflove, *Advances in Computational Electrodynamics : The Finite-Difference Time-Domain Method*; Artech House, Boston; 1998.
- [2] David M. Hockanson, James L. Drewniak, Todd H. Hubing & Thomas P. Van Doren, “FDTD modeling of common-mode radiation from cables,” *IEEE Trans. Electromagn. Compat.*, vol. 38, pp. 376-387, August 1996.
- [3] Yuh-Sheng Tsuei, A. C. Cangellaris and J. L. Prince, “Rigorous electromagnetic modeling of chip-to-package (first-level) interconnections,” *IEEE Trans. Components Hybrids Manuf. Technol.* vol. 16, pp.876-882, December 1993.
- [4] J. Gilbert and R. Holland, “Implementation of the thin-slot formalism in the finite-difference EMP code THREDII,” *IEEE Trans. Nucl. Sci.*, vol. NS-28, pp. 4269-4274, December 1981.

- [5] M. Li, K-P. Ma, J. L. Drewniak, T. H. Hubing, and T. P. Van Doren, "Numerical and experimental corroboration of an FDTD thin-slot model for slots near corners of shielding enclosures", *IEEE Trans. Electromagn. Compat.*, vol. 39, pp. 225-232, August 1997.
- [6] J. P. Berenger, "Perfectly matched layer for the absorption of electromagnetic waves," *J. Comput. Phys.*, vol. 114, pp. 185-200, October 1994.
- [7] W. L. Ko and R. Mittra, "A comparison of FD-TD and Prony's methods for analyzing microwave integrated circuits", *IEEE Trans. Microw. Theory Tech.*, vol. 39, pp.2176-2181, December 1991.
- [8] M. Li, J. Nuebel, J. L. Drewniak, T. H. Hubing, R. E. DuBroff and T. P. VanDoren, "EMI from airflow aperture arrays in shielding enclosures--experiments, FDTD and MoM modeling", submitted to *IEEE Trans. Electromagn. Compat.*
- [9] C. M. Butler, Y. Rahmat-Samii, R. Mittra, "Electromagnetic penetration through apertures in conducting surfaces", *IEEE Trans. Antennas Propagat.*, vol. 26, pp.82-93, January 1978.
- [10] S. M. Rao, D. R. Wilton, A. W. Glisson, "Electromagnetic scattering by surfaces of arbitrary shape", *IEEE Trans. Antennas Propagat.*, vol.30, pp.409-418, May 1982.
- [11] D. Morgan, *A Handbook for Testing and Measurement*; Peter Peregrinus Ltd., on behalf of IEE; 1994.
- [12] T. Y. Otoshi, "A study of microwave leakage through perforated plates", *IEEE Trans. Microw. Theory Tech.*, vol.20, pp.235-236, March 1972.
- [13] H. A. Bethe, "Theory of diffraction by small holes", *Physical Review*, vol. 66, pp.163-182, 1944.